Prediction of capacity for moment redistribution in FRP-strengthened continuous RC T-beams

Abbas Tajaddini[1, 6], Tim Ibell[2], Antony Darby[3], Mark Evernden[4], and Pedro Silva[5]

[1] Research assistant, Department of Architecture and Civil Engineering, University of Bath, UK, BA2 7AY
[2] Professor, Department of Architecture and Civil Engineering, University of Bath, UK
[3] Reader, Department of Architecture and Civil Engineering, University of Bath, UK
[4] Senior lecturer, Department of Architecture and Civil Engineering, University of Bath, UK
[5] Professor, School of Engineering and Applied Science, the George Washington University, Washington, USA
[6] Corresponding E-mail address: A.Tajaddini@bath.edu; Tel: +44 1225 385206

Date submitted: 04/04/2016; Word count (including Abstract and References): 7576; Number of figures: 16; Number of tables: 5

ABSTRACT

Due to the premature debonding of fiber-reinforced polymer (FRP) materials which results in a reduction in ductility, the problem of how to exploit moment redistribution (MR) in FRP-strengthened continuous reinforced concrete (RC) structures is still unresolved. To date, limited research has been conducted into MR in such structures, so that a reliable and rigorous solution for quantifying MR throughout the loading cycle remains elusive. This paper aims to quantify MR and predict the capacity at reasonable accuracy, to encourage the use of FRP for the strengthening of existing continuous RC structures. Experiments conducted on twelve continuous T-beams are reported, and the findings are discussed. Strengthening configuration and anchorage scheme are the main variables. A new analytical strategy is described for quantifying MR, and the analytical results are then validated against the experimental results. Both experimental and analytical results confirm that there is no reason to restrict MR into strengthened zones. More importantly, MR out of FRP-strengthened zones can indeed occur, provided that the FRP is sufficiently anchored, and reliable exploitation of this is now possible.

Keywords:

Moment redistribution; continuous members; FRP strengthening; concrete T-beams; FRP anchorage

Introduction

To avoid the need for replacement or demolition of existing reinforced concrete (RC) structures, they are routinely strengthened using various materials and techniques. Research in the literature (Meier et al., 1993; Teng et al., 2001; ACI440-2, 2008) has demonstrated the effectiveness of fiber reinforced polymer (FRP) materials in extending the lifetime of existing RC structures. FRP strengthening of concrete members is known to be a rapid and cost-effective method of strengthening. Thus, FRP is currently used widely for the retrofit of RC structures.

Although FRP can considerably improve the strength capacity of an existing RC structure, previous research (Duthinh and Starnes, 2004; Oehlers, 2006; Yost et al., 2007) has shown that the ductility of RC structures can be reduced after strengthening. The two main reasons for this problem are the elastic nature of FRP which reduces overall curvature ductility of the original member, and the premature and brittle debonding of the FRP from the concrete surface which prevents the ultimate strength of the FRP from being achieved. As a result, the reduction in ductility is considered to affect substantially the degree of moment redistribution which can take place following the FRP strengthening of an existing continuous RC flexural member.

The required level of ductility for moment redistribution (MR) is unclear in FRP-strengthened continuous RC members, and there is a lack of sufficient research to demonstrate a precise level of ductility reduction after adding FRP. Therefore, the exploitation of MR in the design of FRP strengthening systems has been conservatively ignored or restricted by design codes and guides worldwide (e.g. ACI 440.2R, 2008; TR55, 2012). This potentially compromises the safety of such strengthened structures under extreme loads since implication of the lower-bound theorem of plasticity can no longer be relied on for redistribution of load paths. In addition, it should be noted that if MR is ignored in an FRP-strengthened RC member which was originally designed assuming MR, the strengthened member must be necessarily analyzed using elastic equations. Consequently, great quantities of FRP must be added to the member because the fully-elastic situation must now be considered even for the original situation. Therefore, there is a pressing need to investigate fully how MR might be understood and exploited in the strengthening of continuous RC structures.

Potentially, it is difficult and complex to quantify the actual level of ductility, and to predict the capacity for MR when FRP is added to an RC member (Oehlers et al., 2004). Few research studies have experimentally or theoretically investigated redistribution of bending moments in FRP-strengthened RC structures. For example, El-Refaie et al. (2003) tested eleven two-span rectangular beams strengthened using externally bonded (EB) FRP sheet. They found that the quantity and arrangement of the internal steel reinforcement, as well as the quantity of the FRP applied, are the most important factors influencing MR. They recommended that an anchorage system for the FRP should be provided to minimize the risk of premature FRP peeling. They showed significant MR is possible out of strengthened zones, with their particular tests demonstrating up to 35% MR.

In a theoretical study, Oehlers et al. (2004) proposed two approaches, called the 'Flexural rigidity approach' and the 'Plastic hinge approach', to quantify redistribution of bending moments. The two approaches were based on 'stiffness variation' and a 'hinge zone', respectively. They also tested four two-span rectangular slab-shaped concrete beams to measure any possible MR. The beams were strengthened only in the negative zone (over the interior support), using EB CFRP plates. MR up to 35% was found in their particular tests, depending on the arrangement of the internal-steel-reinforcement adopted.

Limited studies have also been conducted by other researchers (Silva and Ibell, 2008; Aiello and Ombres, 2011; Dalfré and Barros, 2011; Breveglieri et al., 2012; Santos et al., 2013; Lou et al., 2015), which show that MR can occur to a significant extent after FRP strengthening, provided that an appropriate strengthening configuration is adopted.

This paper initially presents the findings of a set of experiments, aiming at quantifying MR in FRP-strengthened continuous RC T-beams. Various strengthening configurations and techniques were adopted to evaluate the effect on MR. Twelve two-span RC T-beams were tested in two groups. In addition, the FRP was anchored mechanically in some of the specimens to understand the potential influence of anchorage on the degree of MR. It must be noted that quantification of the effectiveness of the anchorage system itself is not the purpose of this paper. The experimental results are then compared with the analytical results obtained from a novel analytical model developed by the authors (Tajaddini et al., 2013; Tajaddini, 2015). The analytical results is used to quantify the full potential capacity of the tested members for MR, if the FRP were not to debond prior to concrete crushing or FRP rupture.

Moment redistribution (MR)

The implication of MR in statically indeterminate structures has been described in the literature (Bondy, K.B., 2003; Oehlers et al., 2010; Bagge et al., 2014) through simple examples. RC structures are designed so that they resist external actions elastically within the serviceability load range. Beyond this range, if one (or more) section of the structure reaches its moment capacity, the section will rotate at a constant bending moment, forming a plastic hinge provided that the section has sufficient ductility. As shown in Fig. 1, an idealized elastic-plastic relationship between curvature and bending moment is assumed in an unstrengthened ductile section, in which M_{cr} is the bending moment at first cracking, M_u is the ultimate moment capacity, φ_y is the curvature at steel yielding, φ_u is the ultimate curvature, and EI is the uncracked flexural stiffness. Now, as the applied load is further increased, the critical point (plastic hinge location) will redistribute the extra bending moment to other parts of the structure to accommodate the increase in loading.

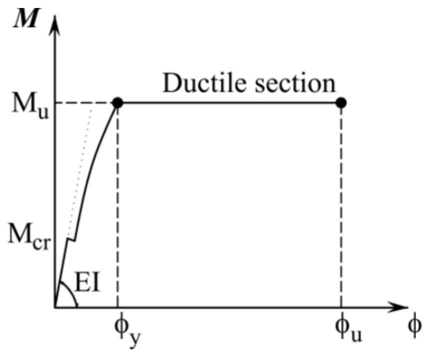

Fig. 1. *An idealized elastic-plastic Moment-Curvature relationship in a ductile RC section*

The redistribution of bending moment continues, and plastic hinges are formed successively in the structure, until a failure mechanism is formed and the structure collapses. Through this process, the structure withstands extra applied loads after yielding of the first section until the structure collapses ultimately. In the case of sufficient ductility, the initial elastic bending moment diagram can be significantly different from the final redistributed bending moment diagram at ultimate failure. Therefore, the ratio of the negative bending moment to positive bending moment does not remain constant. As described by El-Refaie et al. (2003), the amount of MR is calculated at each applied load increment (up to failure) using the following equation:

$$\boldsymbol{MR}\ (\%) = \mathbf{100} \times \left(\mathbf{1} - \frac{\boldsymbol{M_{redistributed}}}{\boldsymbol{M_{elastic}}}\right) \qquad (1)$$

where $M_{redistributed}$ is the redistributed bending moment at a critical location at the applied load, and $M_{elastic}$ is the theoretical elastic bending moment determined from elastic analysis at the same location, assuming an initial uncracked elastic flexural stiffness.

MR becomes a complex problem when FRP is added to a continuous RC beam. As illustrated in Fig. 2, an FRP-strengthened continuous RC beam might have various zones which can be unstrengthened (e.g. Zone A), lightly strengthened (e.g. Zone B), or heavily strengthened (e.g. Zone C). Over the loading cycle, each zone experiences a specific level of stiffness variation which is different from other zones.

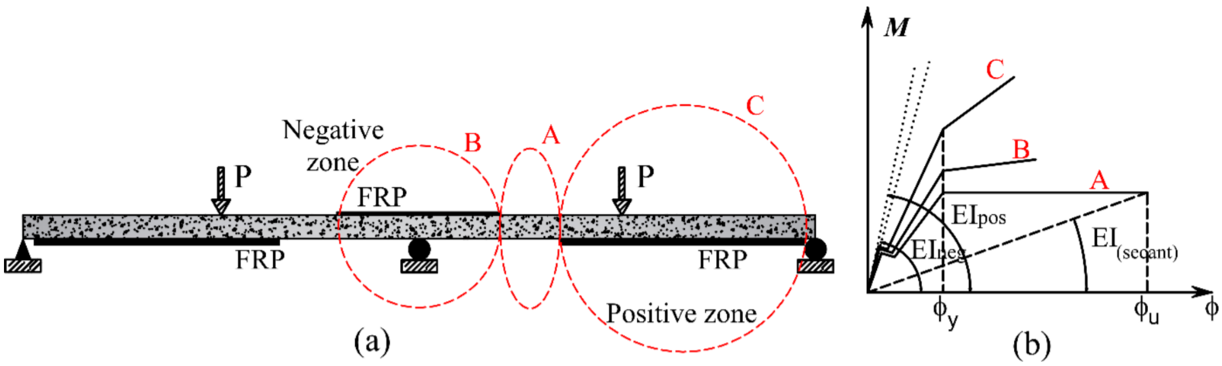

Fig. 2. *(a) Schematic image of a continuous FRP-strengthened beam; and (b) Moment-Curvature relationships for different zones of the beam*

As illustrated schematically in Fig. 2(b), a lack of horizontal plastic plateau in the Moment-Curvature relationship of the FRP-strengthened zones (zones B and C) prevents plastic hinges forming in the strengthened zones. This is because the FRP resists the applied load linearly until failure, even if the steel reinforcement yields before FRP failure. The complexity of quantifying MR becomes greater if various amounts of FRP are added to different parts of a concrete member. Applying various strengthening configurations and techniques with different anchoring schemes affects the flexural behavior and failure mode of the strengthened member. All these indicate that a comprehensive investigation of the problem is still required.

Experimental study

Test aim and program

A set of experiments were designed to examine the effect of FRP strengthening on the level of MR in continuous RC flexural members. The test aims included:

- To experimentally investigate MR in RC continuous T-beams when strengthened using FRP, as standalone rectangular beams are rarely found in reality;
- To examine the influence of various strengthening techniques and configurations on MR;
- To verify the new analytical model developed by the authors previously for quantifying MR;
- To understand the effect of FRP anchorage on the level of MR.

Test specimens were two-span and loaded at one of the mid-span points, using a concentrated load. This specific load arrangement caused the beam to only have one positive zone and one negative zone along its length. Therefore, this means that MR could only occur from one zone to the other (either from the positive zone to the negative zone or vice versa), ensuring MR could be easily tracked and quantified while still allowing different strengthening strategies to be explored. In addition, this asymmetrical arrangement of loading allowed the analytical model to be verified in a general sense as, for example, in the numerical procedure it would not matter whether rotation was zero or not at the position of central support. Twelve T-beams were designed and cast in two groups of T and U. Group T included six test specimens positioned in the usual upright T configuration, as shown in Fig. 3. Group U included six test specimens positioned upside-down so that MR could be studied comprehensively into and out of asymmetric sections. The main variables included configuration of the FRP strengthening and anchorage. The soffit of the positive zone of the specimens, under the load position, was strengthened (where applicable) using the externally bonded (EB) FRP plate, while the negative zone, over the central support, was strengthened (where applicable) using near surface mounted (NSM) FRP tape embedded into the surface of the flange. The NSM technique was used as a column would be in the way in reality, and it would be impossible to use the EB FRP plate or sheet for strengthening of such zones. Fig. 3 illustrates a schematic image of the geometry, loading arrangement and cross-section of the beams in group T. All specimens were designed such that they could exhibit up to 30% MR before FRP strengthening, as recommended by design guidelines such as BS 8110-1 (2005), AS 3600 (2009), and CSA A23.3 (2014) for conventional RC members. Note that, ACI-318 (2014) limits MR to 20% in such members, but the reality is that more MR can be achieved.

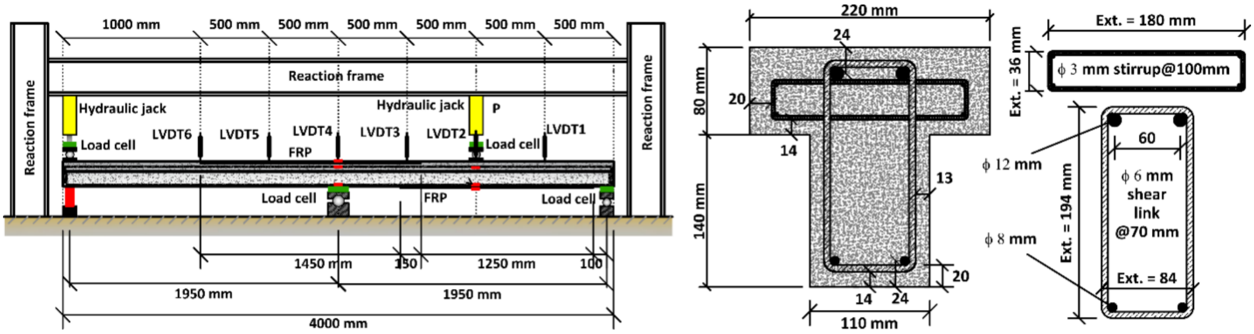

Fig. 3. Geometry, load arrangement and cross-section of the T-beams in group T

Since the positive and negative bending moments were so different over the loading cycle due to the specific loading arrangement adopted, MR was only possible in one direction (i.e. from the positive zone to the negative zone). Therefore, as the positive zone was only strengthened with the EB technique, it would not be possible to quantify MR out of the negative zone which was strengthened with the NSM technique. To solve this problem and to examine the effectiveness of the NSM technique in redistribution of bending moment, the "upside-down" Group U was designed in order to quantify experimentally bending moment redistributed out of NSM-strengthened zones.

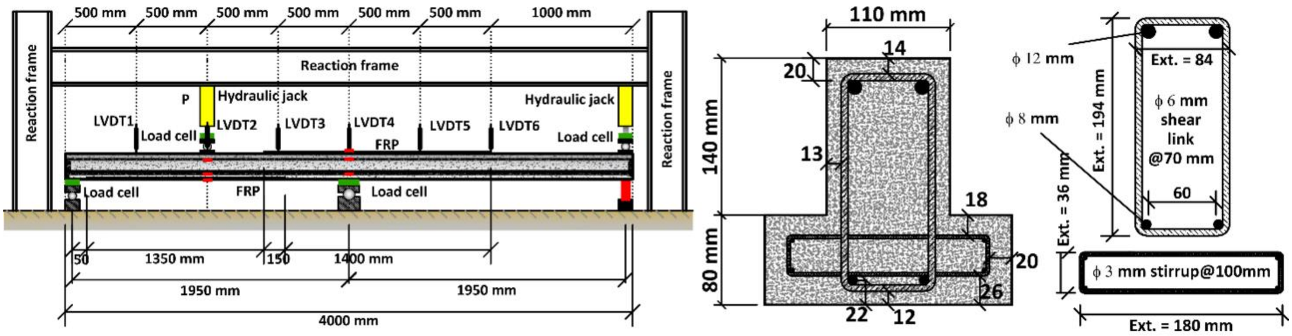

Fig. 4. Geometry, load arrangement and cross-section of the T-beams in group U

The overall length of the specimens was 4000 mm, and each span was 1950 mm long. A single concentrated load was applied at a distance of 1000 mm from the central support. Each beam had a 220-mm flange width, 220-mm height, 110-mm web width, and 80-mm flange depth. The beams were internally reinforced using two longitudinal 12-mm diameter steel bars at the top, and two longitudinal 8-mm diameter steel bars at the bottom of the section. These steel quantities were chosen to encourage high levels of potential MR 6mm-diameter stirrups were used in the web, spaced at 70-mm centers, to prevent shear failure. The flange was also reinforced against shear using 3mm-diameter stirrups, spaced at 100 mm centers.

Deflections of the test specimens were recorded continuously during the testing, using six Linear Variable Differential Transformers (LVDTs) placed on top of the beams (as shown in Figs. 3 and 4). Values of the applied load and support reactions were also recorded over the loading cycle, using digital load cells. Therefore, bending moments in both critical positive and negative zones could easily be calculated. Electrical resistance strain gauges (shown as small solid blocks in Figs. 3 and 4) were installed on the tension and compression steel reinforcement and on the FRP in both positive and negative zones to record strains, and to monitor the flexural softening of both zones during loading. A hydraulic jack was used on top of the exterior support in the unloaded (right-hand) span to prevent it moving upward, and a locked-off jack was also used below the specimens for ease of adjustment.

Table 1 summarizes specifications of the specimens in the two groups. Different strengthening configurations were adopted for the experiments to assess the degree of bending moment which could be redistributed into and out of the strengthened zones. One specimen was used as the control specimen in each group (i.e. T1 and U1). Beams T2 and T3 were strengthened only in the positive zone using EB carbon FRP plate. Beam T4 was strengthened only in the negative zone using NSM carbon tape. Beams T5 and T6 were strengthened in both the positive and negative zones using EB carbon plate and NSM tape, respectively. Beam U2 was strengthened only in the positive zone using NSM carbon tape. Beams U3 and U4 were strengthened only in the negative zone using EB carbon FRP plate. Beams U5 and U6 were strengthened in both the positive and negative zones using NSM tape and EB carbon plate, respectively.

Table 1. Specifications of the test specimens

Beam	Positioning type	Strengthening configuration	Strengthening system	EA value of FRP (kN)	Anchorage system	f_c^* (MPa)
T1	Normal	Control (no FRP)	N/A	-	N/A	35.6
T2	Normal	Positive zone	CFRP plate	9900	-	29.1
T3	Normal	Positive zone	CFRP plate	9900	U-wrap	36.1
T4	Normal	Negative zone	NSM CFRP tape	9100	-	27.3
T5	Normal	Both positive and negative zones	CFRP plate (Pos)	9900	-	32.6
			NSM tape (Neg)	9100		
T6	Normal	Both positive and negative zones	CFRP plate (Pos)	9900	U-wrap	35.3
			NSM tape (Neg)	9100		
U1	Upside-down	Control (no FRP)	N/A	-	N/A	34.7
U2	Upside-down	Positive zone	NSM CFRP tape	9100	-	35.7
U3	Upside-down	Negative zone	CFRP plate	9900	-	29.2
U4	Upside-down	Negative zones	CFRP plate	9900	U-wrap	32.5
U5	Upside-down	Both positive and negative zones	CFRP plate (pos)	9900	-	31.6
			NSM tape (neg)	9100		
U6	Upside-down	Both positive and negative zones	CFRP plate (pos)	9900	U-wrap	30.3
			NSM tape (neg)	9100		

Note: $^*f_c$ = Average cylinder compressive strength of concrete on the day of testing.

FRP anchorage system

To anchor the EB FRP plates mechanically, U-wrap anchors were used in beams T3, T6, U4 and U6. The U-wraps were installed at an inclination of 45^0, as research (Lee, 2010) has shown that the anchors are more effective in this direction than when vertical, to improve bond strength between the concrete and the FRP. Each anchor was made of carbon FRP sheet, and consisted of two similar pieces. Figs. 5(a) and (b) illustrate schematic images of the U-wraps installed on the soffit of the beams in group T, and over the central support in group U, respectively.

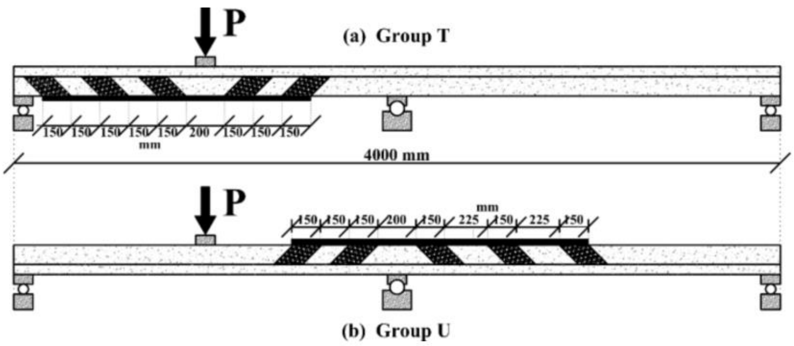

Fig. 5. *The U-wrap anchors used for the FRP plates. (a) Group T; (b) Group U*

The U-wraps were distributed along the entire length of the FRP plate, to help ensure the carbon plate would remain fully attached to the concrete along the full length during testing.

Material properties

Each specimen was cast separately using a manual concrete mixer. The compressive strength of concrete was measured for each beam on the day of testing through crushing standard cylinders of 100 mm-diameter × 200-mm height. The measured values are summarized in Table 1. Also, properties of the steel reinforcements used are listed in Table 2 for the four different sizes of 3 mm, 6 mm, 8 mm and 12 mm.

Table 2. Mechanical properties of the steel reinforcement

Steel bar diameter (mm)	Yield strength, f_y (MPa)	Ultimate strength, f_u (MPa)	Young's modulus, E_s (GPa)
3 (High yield smooth shear links)	710	768	213
6 (High yield ribbed shear links)	568	630	200
8 (High yield deformed bars)	575	633	200
12 (High yield deformed bars)	573	652	200

The CFRP material used for strengthening of the beams was a precured unidirectional plate of 1.4 mm thick × 50 mm wide. In addition, a precured carbon tape of cross-sectional area of 2 mm × 16 mm was adopted to strengthen the beams using the NSM method. The CFRP sheet used for the U-wraps was high-strength, unidirectional of 0.16 mm nominal thickness. The carbon sheet was applied to the beams by the wet-layup method, and impregnated in place using a two-part epoxy resin (Sikadur-330). The CFRP plate and tape were installed using a two-part epoxy structural adhesive (Sikadur-30). Average mechanical properties of the FRP materials measured through conducting unidirectional tensile testing on three samples, and of the epoxy resins provided by manufacturers, are listed in Table 3.

Table 3. Mechanical properties of the strengthening materials

Material	Ultimate tensile strength (σ_f)	Tensile modulus (E_f)	Ultimate strain (ε_{fu})	Bond strength
CFRP sheet	4230 MPa	238 GPa	1.78 %	N/A
CFRP plate	2590 MPa	145 GPa	1.79 %	N/A
CFRP tape	2410 MPa	141 GPa	1.68 %	N/A
Epoxy resin (Sikadur-330)	30 MPa	4.5 GPa	0.9 % (7 days)	> 4 MPa
Epoxy resin (Sikadur-30)	26-31 MPa	11.2 GPa	1.0 % (7 days)	> 4 MPa

Test results

Modes of failure

The unstrengthened control specimens, T1 and U1, failed in a conventional ductile manner, as expected for an under-reinforced RC flexural member, through concrete crushing following yielding of the tension steel reinforcement. Due to the loading arrangement adopted, the negative zone failed after initial plastic yielding of the positive zone. Figs. 6(a) and (b) show respectively the positive and negative zones of beam U1 at ultimate failure, when a plastic hinge has been formed in the negative zone following the earlier formation of a plastic hinge in the positive zone. The major test results and findings are provided in Table 4 for all test specimens.

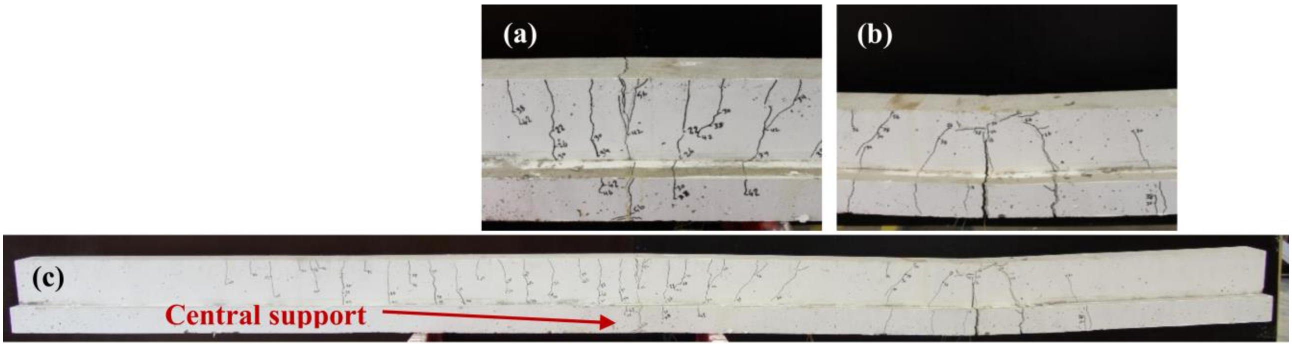

Fig. 6. *Failure of beam U1: (a) Negative zone; (b) Positive zone; (c) Entire beam*

Table 4. Experimental results of the specimens

Beam	Failure mode	Anchorage	P_{cr} (kN)	$P_{y\text{-}P}$ (kN)	$P_{y\text{-}N}$ (kN)	P_u (kN)	ε_{deb}	P_R (kN)	MR (%)
T1	Concrete crushing	-	14	34	54	54	-	-	34
T2	FRP debonding	-	16	53	-	54	0.35 %	-	7
T3	FRP debonding	U-wrap	16	55	54	104	1.20 %	55	10
T4	FRP debonding	-	14	32	65	71	0.90 %	54	48
T5	FRP debonding	-	18	54*	65	53	0.35 %	71	9
T6	FRP debonding	U-wrap	18	63	-	114	1.20 %	55	13
U1	Concrete crushing	-	13	33	55	55	-	-	32
U2	FRP debonding	-	17	54	64	94	1.50 %	55	11
U3	FRP debonding	-	14	32	55*	62	0.35 %	56	42
U4	FRP debonding	U-wrap	14	33	66	72	0.90 %	55	52
U5	FRP debonding	-	19	58	83	92	1.00 %	85	18
U6	FRP debonding	U-wrap	20	61	83	106	1.40 %	83	20

Note: P_{cr} = Load at which first cracking occurred; P_u = Failure load (at FRP debonding);
$P_{y\text{-}P}$ = Yield load of the positive zone; $P_{y\text{-}N}$ = Yield load of the negative zone;
ε_{deb} = Debonding strain of FRP; *After FRP debonding
P_R = Residual load capacity (indicating the ultimate load capacity after FRP debonding and before final concrete crushing);
MR = Experimental MR out of positive zone at failure

In all strengthened beams, FRP debonding occurred prior to any other form of failure, and signaled in every case the peak capacity. The tension reinforcement in the positive zone yielded prior to FRP debonding in all cases. As described in Table 4, the carbon plate debonded at applied loads of 54 kN and 104 kN in beams T2 and T3, respectively. This demonstrated that the application of U-wraps was successful and effective such that the load resistance doubled, and the debonding strain was improved from 0.35% in beam T2 to 1.2% in beam T3.

The NSM tape in beam U2 debonded at an applied load of 94 kN. A large strain of 1.5% was recorded in the NSM tape at failure, demonstrating the effectiveness of using the NSM technique for strengthening of RC beams compared with other methods where ductility is required. The high bond strength between the concrete and FRP is obtained in the NSM technique due to the FRP being fully surrounded by epoxy resin. Debonding of the FRP in specimens T2, T3 and U2 is shown in Fig. 7.

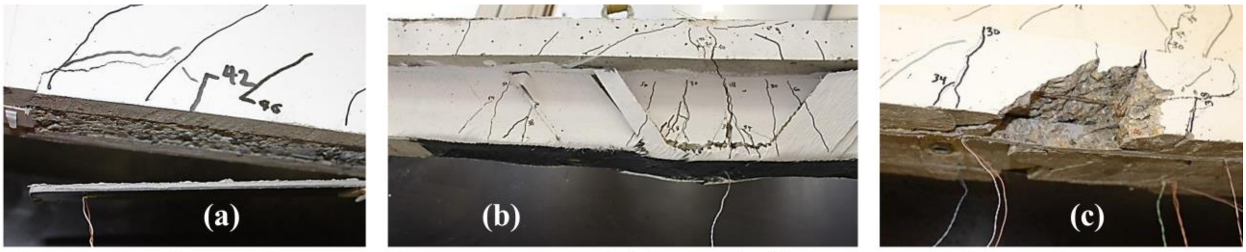

Fig. 7. *Debonding of the FRP in the positive zone: (a) beam T2; (b) beam T3; (c) beam U2*

Fig. 8 shows debonding of the FRP in beams T4, U3 and U4. The NSM tape in beam T4 debonded at an applied load of 71 kN. The strain recorded in the NSM tape at debonding was 0.9%, demonstrating a better bond performance between concrete and the FRP compared with that of EB FRP plates. The carbon plate debonded at applied loads of 62 kN and 72 kN in beams U3 and U4, respectively. The strains recorded in the FRP at debonding were 0.35% and 0.9% respectively, indicating the effectiveness of the U-wraps in postponing debonding, and improving the ductility of the strengthened section in beam U4, compared with that of beam U3.

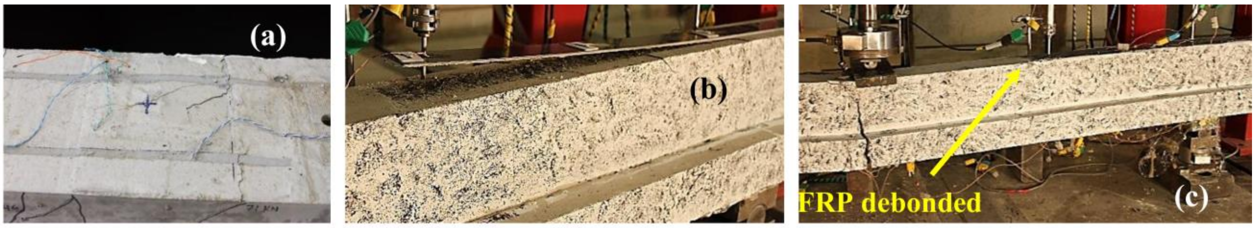

Fig. 8. *Failure of the FRP in the negative zone: (a) beam T4; (b) beam U3; (c) beam U4*

The specimens strengthened in both the positive and negative zones (i.e. T5, T6, U5 and U6) exhibited a linear flexural behavior up to steel yield, and a partially ductile behavior after yielding of the steel reinforcement in the positive zone until FRP debonding. All four beams failed first in the positive zone through FRP debonding which occurred after steel yield. The negative zone failed later through the same failure mechanism. Fig. 9 depicts failure of the FRP in beams T5, T6, U5 and U6. The carbon plate in the positive zone debonded at applied loads of 53 kN and 114 kN in beams T5 and T6, respectively. The ultimate strains recorded in the FRP plate at debonding were 0.35% and 1.2% in the two beams, respectively. In beams U5 and U6, the NSM tape in the positive zone debonded at applied loads of 92 kN and 106 kN, respectively. Strains of 1% and 1.4% were recorded in the FRP tapes at debonding in the two beams. The load was further increased until the FRP plate in the negative zone debonded at 85 kN and 84 kN in beams U5 and U6, respectively. The debonding strain was 0.35% in beam U5, but it was 0.85% in beam U6 due to the application of U-wraps.

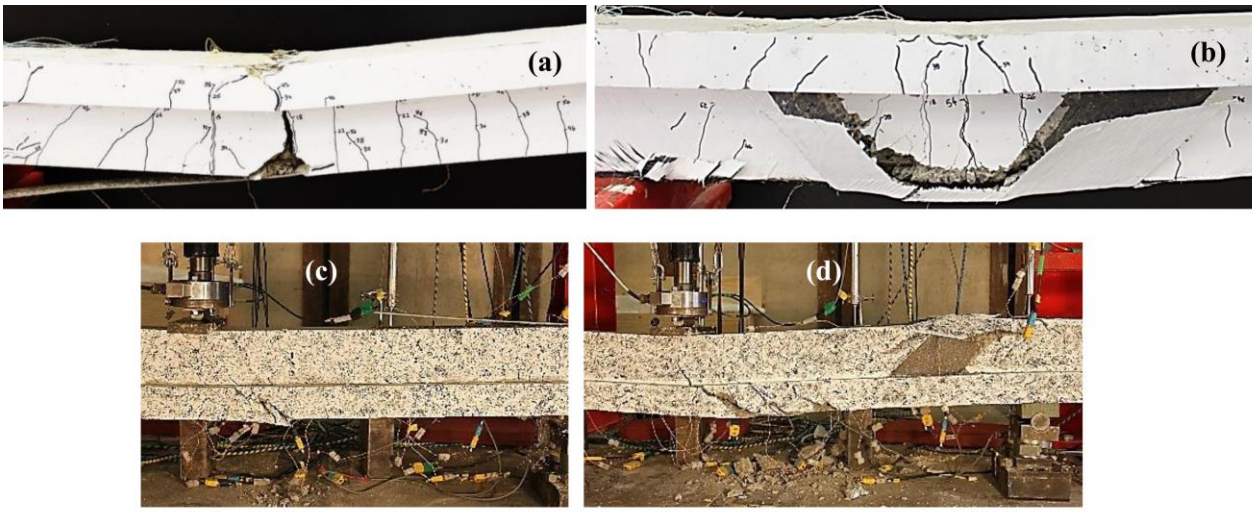

Fig. 9. *Failure of the FRP in critical zones: (a) beam T5; (b) beam T6; (c) beam U5; (d) beam U6*

As shown in Table 4, FRP strengthening of RC structures improves the load capacity of the structure provided that the FRP does not debond prematurely at a low strain. The effectiveness of strengthening was higher when the FRP was added to the positive zone. This was due to the loading arrangement adopted. The failure load increase ratio (λ) shows that the increase in load capacity could be from 67% to 111% when the positive zone was strengthened. As shown later in Figs. 10 and 11, ductility of the beams became higher when the negative zone only was strengthened.

Load-Deflection response

Ductility of RC beams can be evaluated by measuring the deflection of critical points over the loading cycle (Mukhopadhyaya, 1998). Figs. 10 and 11 show the relationships between the applied load and mid-span deflection in the loaded span, recorded by LVDT2 (as depicted in Figs. 3 and 4) for the beams in group T and U, respectively. Three major phases are observed in the Load-Deflection relationships including the linear-elastic phase (from the beginning of loading to first concrete cracking), the cracked-elastic phase (from concrete cracking to yielding of the tension steel reinforcement), and the plastic phase (from steel yield to FRP debonding or concrete crushing).

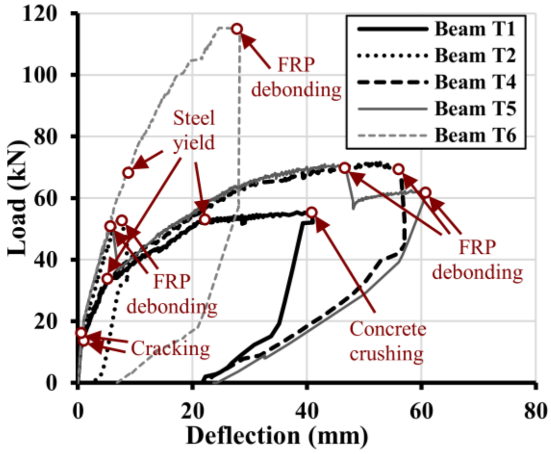

Fig. 10. *Load-Deflection relationships for the beams in group T*

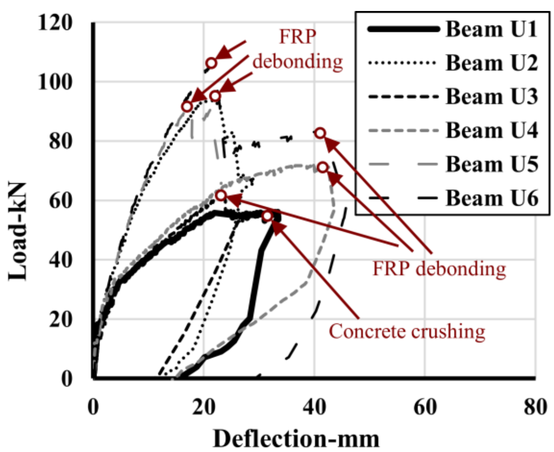

Fig. 11. *Load-Deflection relationships for the beams in group U*

Load-Strain response

Figs. 12 and 13 show the relationships between the applied load and strain in the FRP for the beams in groups T and U, respectively. Strain behavior of the unanchored FRP plate at the mid-span of beam T5 is similar to that of beam T2, and strain behavior of the anchored plate at the mid-span of beam T6 was similar to that of beam T3. After first concrete cracking, strain of the FRP increased considerably, and subsequently, the strain increased again after steel yield when a significant reduction in stiffness occurred. Comparison of the ultimate strain in the FRP plate between beams T2 and T3, between beams T5 and T6, between beams U3 and U4, and between beams U5 and U6 demonstrates the effectiveness of U-wrap anchors in improving the bond performance between concrete and the FRP plate.

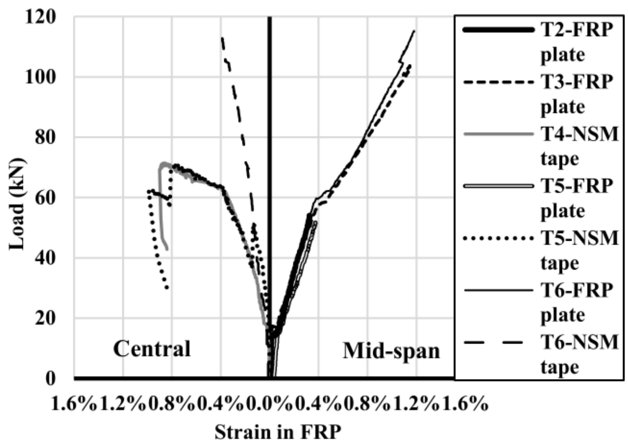

Fig. 12. *Load-Strain relationship in the FRP for the beams in group T*

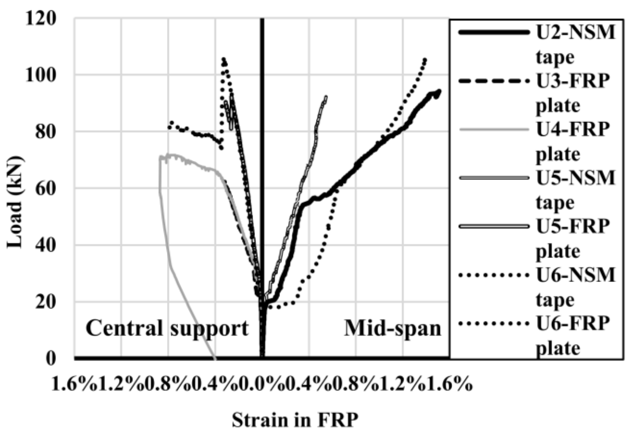

Fig. 13. *Load-Strain relationship in the FRP for the beams in group U*

Moment redistribution

The bending moment redistributed out of the positive zone and into the negative zone at failure has been quantified at each load increment using Eq. (1). The values of experimental MR out of the positive zone at failure for all beams are listed in Table 4. The hypothetical elastic bending moment at failure (M_{elas}) was calculated using elastic analysis, assuming no MR occurred and that the ultimate loading condition led to an entirely elastic distribution of bending moment.

The unstrengthened beams in both groups (T1 and U1) exhibited 34% and 32% MR at failure, respectively. As shown in Table 4 and later in Figs. 15 and 16, bending moment was redistributed without limit into FRP-strengthened zones during the experiments. The flexural behavior of the specimens strengthened only in the negative zone (i.e. T4, U3 and U4) was ductile (i.e. the internal steel yielded sufficiently) during loading despite being strengthened with FRP. This can be seen from Figs. 10 and 11, also from the percentage of MR at failure given in Table 4, compared with that of the control beams.

Although limited, it was found that bending moment was redistributed out of FRP-strengthened zones by up to 20% in these particular tests. The flexural behavior of the specimens strengthened only in the positive zone (i.e. T2, T3 and U2) was almost linear-elastic up to FRP failure. The ratio of positive moment to negative moment was destined to remain constant in the three beams where the FRP had been added to the positive zone in a large quantity so that the limits of bending strength in both zones were reached nearly simultaneously. This prevented significant MR from needing to occur. Adding FRP to the positive zone in beams T2 and U2 caused a considerable reduction in the level of MR compared with that found in beams T1 and U1. In fact, the addition of elastic FRP resulted in 7%, 10% and 11% MR out of the strengthened zone in beams T2, T3 and U2 respectively.

Overall, the beams strengthened in the positive zone (i.e. T2, T3, T5, T6, U2, U5 and U6) exhibited lower capacity for MR than the specimens strengthened only in the negative zone (i.e. T4, U3 and U4). The difference between amounts of MR in beams T2 and T3, in beams T5 and T6, and in beams U3 and U4 indicates the effectiveness of FRP anchorage. Moreover, the difference of MR between beams T2 and U2, and between T6 and U6 can somewhat demonstrate the advantage of the NSM technique on the EB technique in improving ductility. The experimental findings in general demonstrate that the amount of redistribution depends on the FRP stiffness (EA value) and quantity, method of installation, strengthening configuration, anchoring scheme and, of course, the precise geometry of the structure and loading conditions.

Analytical model

The authors have previously proposed and developed a new analytical model to quantify MR in FRP-strengthened RC flexural members rigorously (Tajaddini et al., 2013; Tajaddini, 2015). The model is a novel theoretical strategy which employs basic structural mechanics to track MR, without any need for estimating rotation capacity or curvature ductility. Redistribution of bending moment in a beam is quantified through finding and updating the variation of flexural stiffness along the length of the beam over the loading cycle. Briefly, the model uses a numerical technique in which the beam is subdivided into a large number of vertical segments. Based on constitutive relationships, the Moment-Curvature plot is determined for each section using equilibrium of forces. Then, at each load increment, the flexural stiffness of each section along the beam is calculated from the Moment-Curvature relationship. An iterative approach is then used to find the actual distribution of bending moment along the beam, by including the effects of stiffness variation at each section and at each step. After each iteration, the flexural stiffness is updated for each section across the structure. The degree of MR can be determined at any point along the beam length, and at any stage of loading, until failure. The analytical model allows the flexural behavior of continuous FRP-strengthened RC beams, even if nonlinear, to be predicted. In addition, a wide variety of beam geometry, loading arrangement and strengthening technique or configuration can be considered. In this section, the analytical model is validated against the findings obtained from the experimental study on groups T and U.

The curvatures at the critical sections were calculated through the experimental data collected using the strain gauges installed on the steel reinforcement and FRP in the negative and positive zones. Fig. 14 illustrates a schematic image of the analytically predicted MR at failure in beam T1. The difference between the solid line (redistributed actual bending moment distribution at failure) and the dashed line (an elastic estimation of bending moment distribution at failure assuming no MR) shows graphically the degree of MR at failure along beam T1, based upon analytical results.

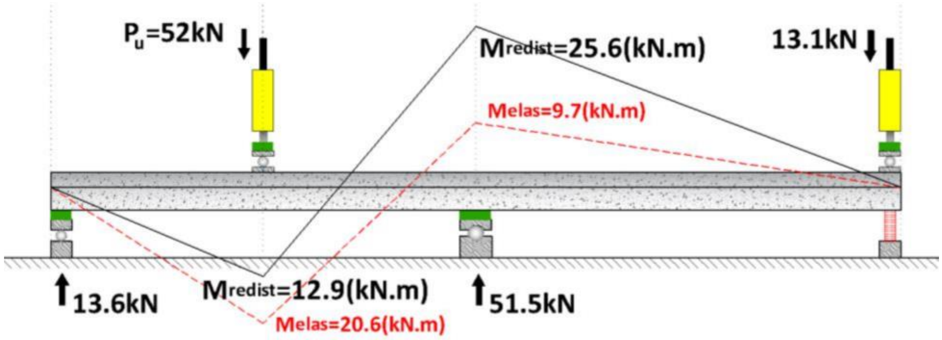

344 ***Fig. 14.*** *A schematic image of MR at failure in beam T1*

345 Figs.15 and 16 illustrate the relationship between the applied load and bending moments in the positive and
346 negative zones throughout loading for the beams in groups T and U respectively.

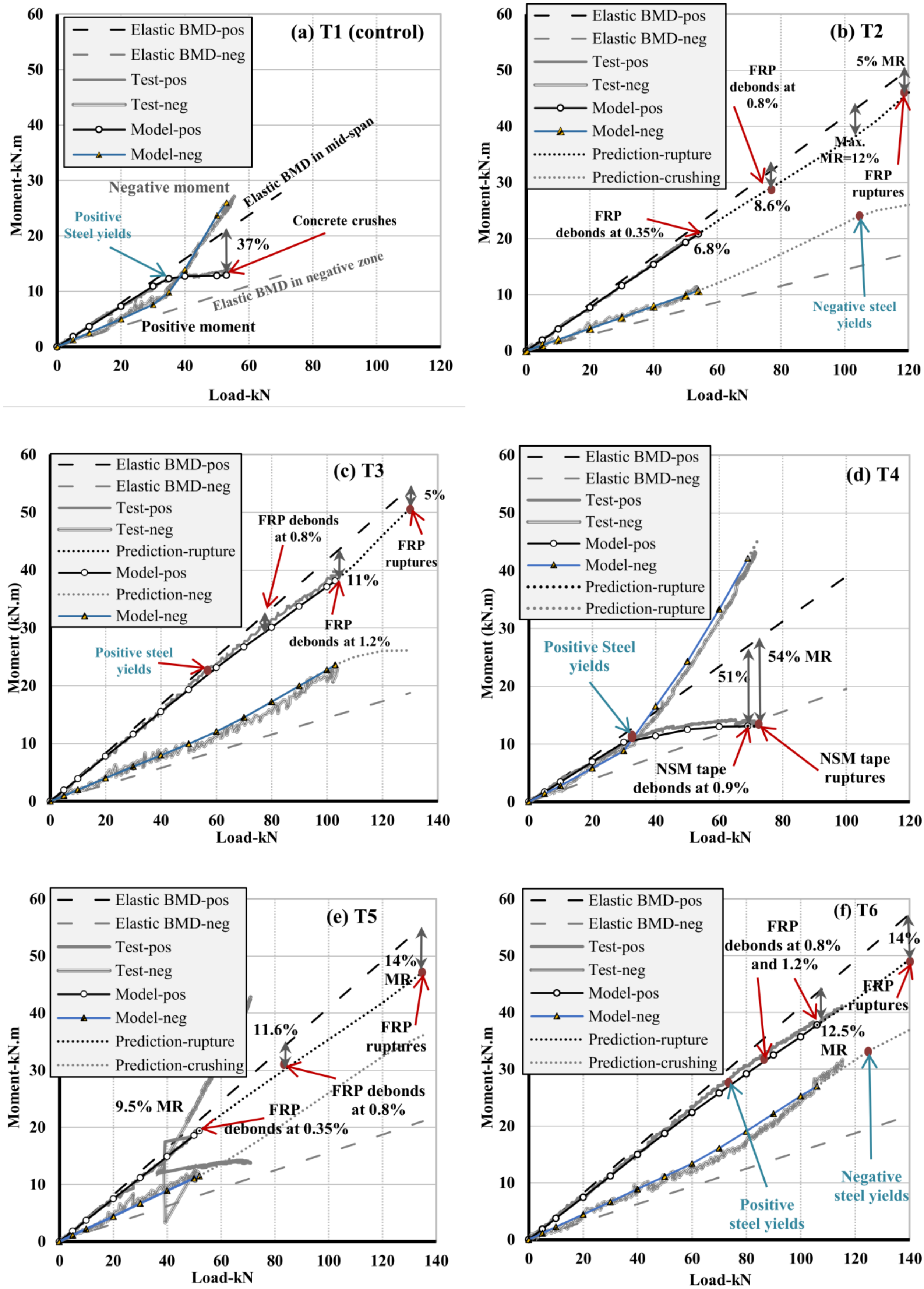

Fig. 15. Experimental Load-Moment curves vs analytical predictions for the beams in group T

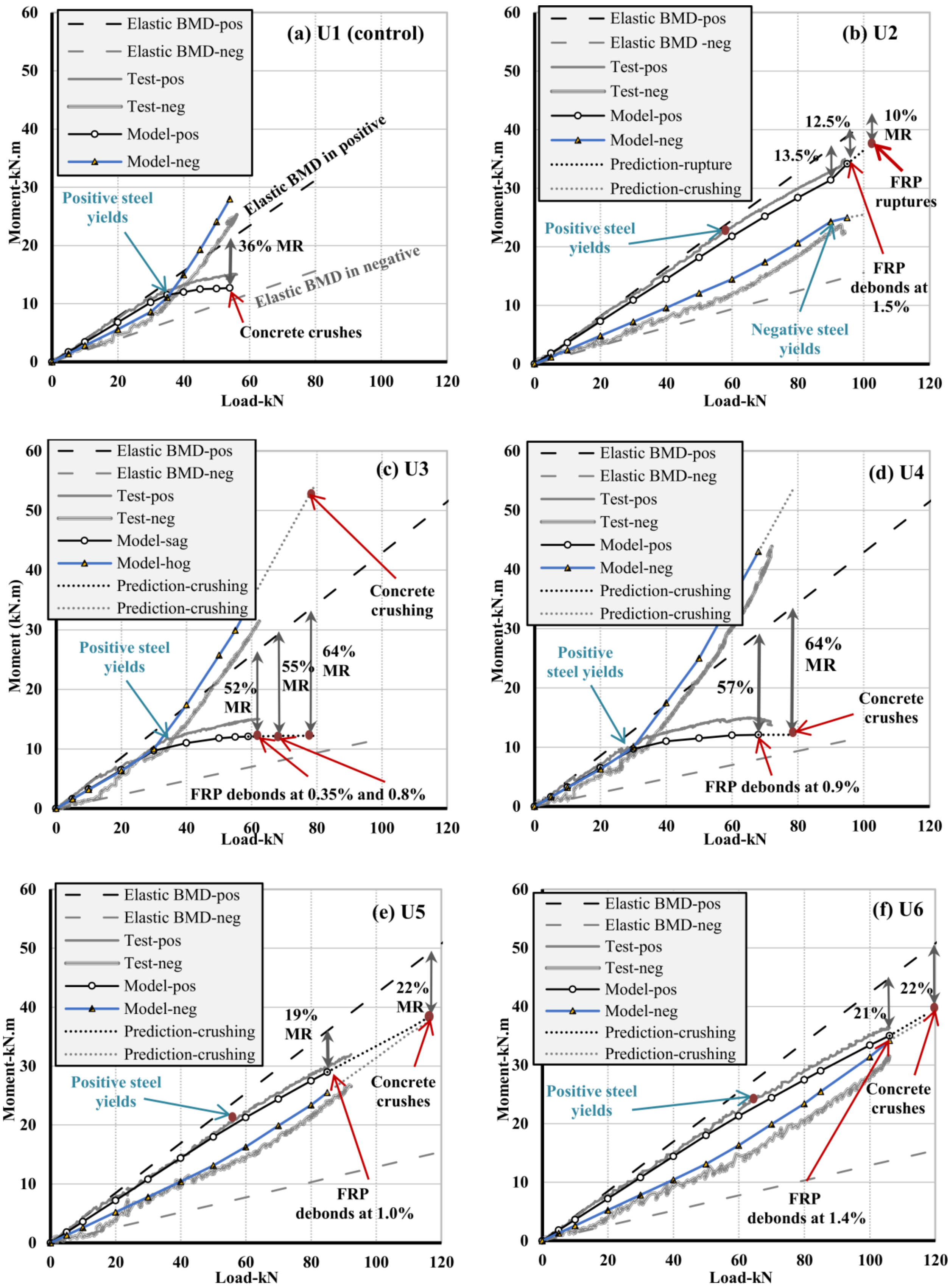

348 ***Fig. 16.*** *Experimental Load-Moment curves vs analytical predictions for the beams in group U*

349

Comparison and discussion

A good correlation can be seen between the experimental and analytical results for all tested beams in Figs. 15 and 16. This indicates how accurate the analytical model can predict the flexural behavior of FRP-strengthened RC structures from the beginning until failure. A brief comparison of the experimental and analytical results is provided in Table 5.The analytical predictions for MR in beams T1 and U1 were 37% and 36%, respectively. The analytical model shows predictions of 7% and 13% for MR in beams T2 and U2 at the same debonding strain recorded experimentally. If the FRP debonded at a typical strain of 0.8% (according to TR55, 2012), predictions for MR would be 9% and 8%, respectively.

Table 5. Summary of the result comparison for the tested beams

Beam	Strengthening location	Anchorage system	Experimental failure load (kN)	Analytical failure load (kN)	MR_E (%)	MR_{An} (%)	$MR_{0.8}$ (%)	MR_{max} (%)
T1	N.A (control)	-	54	52	34	37	-	37
T2	Positive zone	-	54	54	7	7	9	12
T3	Positive zone	U-wrap	104	103	10	11	9	12
T4	Negative zone	-	71	69	48	51	50	54
T5	Both zones	-	52	52	9	10	12	14
T6	Both zones	U-wrap	114	106	13	12	11	14
U1	N.A (control)	-	55	54	32	36	-	36
U2	Positive zone	-	94	95	11	13	8	14
U3	Negative zone	-	61	59	42	52	55	64
U4	Negative zone	U-wrap	72	68	52	57	55	64
U5	Both zones	-	92	85	18	19	13	22
U6	Both zones	U-wrap	106	106	20	21	13	22

Note: MR_E = Experimentally recorded MR out of the positive zone;
MR_{An} = Analytical prediction for MR out of positive zone at experimentally recorded debonding strain;
$MR_{0.8}$ = Analytical prediction for MR out of positive zone at a typical debonding strain of 0.8%;
MR_{max} = Maximum possible capacity for redistribution provided that either the FRP ruptures or the concrete crushes;

Anchoring the FRP plate increased the MR from 7% in beam T2 to 10% in beam T3. As shown in Fig. 15(c), the analytical model predicts a failure load of 130 kN, instead of 104 kN recorded experimentally, assuming that the FRP would fail through rupture at its full strain capacity, not debonding. In this case, 5% MR out of the strengthened zone would occur at failure, but the maximum possible capacity for MR would be 11% which occurs at 107 kN at which point the steel reinforcement would yield in the negative zone, and the level of MR out of the positive zone would subsequently be less. Comparison of the results in beams T2, T3 and U2 demonstrates that the NSM technique provides a higher potential for MR than the EB technique even if the EB FRP plate is anchored.

Although it is not significant in the elastic range, MR is initiated after first concrete cracking due to non-uniform stiffness along the length of the beam, and intensifies usually after steel yielding. Beam T4 exhibited 48% MR out of the positive zone which was more than that of the control beam. This demonstrated that adding FRP can even improve the overall ductility of an RC member, provided that a suitable strengthening configuration is adopted. It is predicted that the full capacity for MR in beam T4 would be 54% if the FRP failed through rupture instead of debonding. MRs were 42% and 52% in beams U3 and U4 at failure, respectively. This again indicates the influence of anchoring of the FRP on the level of MR. It is predicted by the model that the full capacity for MR would be 64% in the two beams, which seems rather promising for an FRP-strengthened RC beam.

As can be observed in Table 5, if both critical zones are strengthened, more bending moment can be redistributed compared with the beams strengthened only in the positive zone. However, it is recommended (Denton, 2007) not to strengthen both positive and negative zones together in reality, this configuration was considered here for completeness. Accordingly, beam T5 exhibited 9% MR out of the positive zone at failure, and beam T6 showed 13% MR due to anchoring the FRP plate. It is predicted by the analytical model that the maximum capacity for MR in beams T5 and T6 would be 14%, if the EB FRP plate could reach its full strain capacity of 1.79% before failure.

MR of 18% and 20% occurred out of the NSM-strengthened positive zone in beams U5 and U6, respectively. These significant amounts of redistribution demonstrate that MR can be feasible out of FRP-strengthened zones if an appropriate quantity of FRP is used, and premature debonding of the FRP is prevented. Prediction for full capacity of MR, if debonding can be prevented, is 22% for beams U5 and U6, in which failure would occur through concrete crushing prior to FRP rupture (as shown in Fig. 16(e) and 16(f)). It should be noted that, as the results show, if significant MR is to occur, it is necessary that the internal steel reinforcement should yield, which in turn causes a considerable increase in the curvature of the critical section.

Conclusions

Redistribution of bending moments in FRP-strengthened continuous RC flexural members has been addressed and investigated in this paper both experimentally and analytically. Twelve large-scale concrete T-beams were tested, and an analytical strategy for the quantification of MR was described. The following conclusions are drawn based on the experimental and analytical findings:

- The experimental findings of the current research indicate that an FRP-strengthened zone in an RC member can redistribute bending moment significantly. Up to 20% MR out of strengthened zones was found here. However, this is highly dependent on the initial conditions of the member before strengthening, FRP quantity, configuration and technique of strengthening, and anchoring scheme.

- The new analytical model described here can reasonably model the flexural behavior of FRP-strengthened RC structures such that MR is quantified, at any stage of loading up to failure, at reasonable accuracy.

- Both analytical and experimental results indicate that if only the zone into which bending moment is redistributed is strengthened, the degree of MR in this beam will be higher than that possible in the original unstrengthened beam. This is because the zone from which MR initiates is unstrengthened and ductile, while the strengthened zone has a higher strength compared with that before strengthening. This allows more bending moment to be redistributed into this zone. This is valid even if the FRP debonds at a low strain. Thus, MR into FRP-strengthened zones should be allowed without undue limitations, whereas current design guides and codes can presently be rather conservative in handling this issue.

- If a concrete beam has sufficient capacity originally for MR, the possibility for considerable redistribution of bending moment should not be ignored after FRP strengthening, even out of the strengthened zones. However, if adding FRP causes the ratio of positive bending moment to negative bending moment to be more or less constant over the loading cycle, no (or negligible) MR will be possible.

- An appropriate mechanical anchoring of the FRP can significantly improve ductility of the retrofitted section and, as a result, the degree of MR can increase. The inclined U-wrap anchors exhibited high effectiveness in anchoring the externally-bonded FRP strengthening materials, such that the ultimate strain in the FRP could increase from 0.35% to 1.2% in most cases, which caused up to 10% increase in MR compared with that of the unanchored beam.

- The near surface mounted (NSM) FRP strengthening technique exhibited a more effective structural performance than the externally-bonded FRP plate strengthening technique, with the ultimate strain being larger in the NSM FRP than in the plated FRP. This better performance of the NSM technique was valid even when the FRP plate was anchored mechanically. Hence, it is recommended that the NSM technique is considered when MR is desirable attribute during design.

- The experimental and analytical findings indicate that strengthening of only the zone into which MR occurred was most effective compared with strengthening of both negative and positive zones together in terms of MR. The case when only the zone from which bending moment is redistributed was strengthened was least effective. Failure was catastrophic in the case when both critical zones were strengthened together, compared with that of single-zone strengthening only, such that no residual capacity was observed in the beam after failure of the FRP. In fact, it was observed that the second-critical-zone FRP debonded suddenly and catastrophically, immediately after the first-critical-zone FRP debonded. For this reason, it is recommended that continuous structures are strengthened preferably only in the zones into which MR will occur, and that such redistribution is exploited.

Acknowledgement

Research funding provided by the Engineering and Physical Sciences Research Council (EPSRC: EP/K019015/1; United Kingdom) and the project partners (Concrete repairs Ltd, Fyfe, Highways England, WSP/Parsons Brinckerhoff and Tony Gee and partners) is acknowledged with appreciative thanks. The authors also sincerely appreciate the assistance of the laboratory staff of the Department of Architecture and Civil Engineering at the University of Bath, UK. All data created during this research are openly available from the University of Bath data archive at http://doi.org/10.15125/BATH-00178.

Notations

The following symbols are used in this paper:

E_s = Young's modulus of steel

E_f = Tensile modulus of the FRP

EA = Tension stiffness of the FRP

EI = Flexural stiffness

f_c = Cylinder compressive strength of concrete

f_y = Yield strength of steel reinforcement

f_u = Ultimate strength of steel

M_{elas} = Theoretical bending moment determined from elastic analysis

M_{redis} = Redistributed bending moment

M_{cr} = Bending moment at cracking

M_u = Moment capacity

MR = Moment redistribution

MR_E = Experimental moment redistribution out of positive zone

MR_{AN} = Analytical prediction for moment redistribution at experimental strain

$MR_{0.8}$ = Analytical prediction for moment redistribution at strain of 0.8%

MR_{max} = Maximum capacity for moment redistribution if debonding is prevented

P = Applied load

P_{cr} = Load at concrete cracking

$P_{y\text{-}P}$ = Yield load of positive zone

$P_{y\text{-}N}$ = Yield load of negative zone

P_R = Residual load capacity

P_u = Ultimate (failure) load

ε_{fu} = Ultimate strain

ε_{deb} = Debonding strain

σ_f = Ultimate tensile strength

φ_u = Ultimate curvature

φ_y = Curvature at steel yield

References

ACI 318: 2014, Building Code Requirements for Structural Concrete and Commentary. ACI.

ACI 440.2R: 2008, Guide for the Design and Construction of Externally Bonded FRP Systems for Strengthening Concrete Structures. ACI.

Aiello, M. A., & Ombres, L., 2007. Moment redistribution in continuous reinforced concrete beams strengthened with carbon-fiber-reinforced polymer laminates. *Mechanics of composite materials*, *43*(5), pp. 453-466.

AS 3600: 2009, Australian Standard for the design of reinforced concrete. Standards Australia.

Bagge, N., O’Connor, A., Elfgren, L. and Pedersen, C., 2014. Moment redistribution in RC beams–A study of the influence of longitudinal and transverse reinforcement ratios and concrete strength. *Engineering Structures*, *80*, pp.11-23.

Bondy, K.B., 2003. Moment redistribution: principles and practice using ACI 318-02. *PTI Journal*, *1*(1), pp.3-21.

Breveglieri, M., Barros, J. A., Dalfré, G. M., & Aprile, A., 2012. A parametric study on the effectiveness of the NSM technique for the flexural strengthening of continuous RC slabs. *Composites Part B: Engineering*, 43(4), 1970-1987.

BS EN 1992-1-1: 2004, *Eurocode 2: Design of concrete structures*. General rules and rules for buildings. BSI.

BS 8110: 2005, Structural use of concrete. Code of practice for design and construction. BSI.

Concrete Society Technical Report 55, 2012. *Design guidance for strengthening concrete structures using fiber composite materials*. The Concrete Society, UK.

CSA-A23.3: 2014, Design of concrete structures. National Standard of Canada. CSA.

Dalfré, G., & Barros, J., 2011. Flexural strengthening of RC continuous slab strips using NSM CFRP laminates. Advances in Structural Engineering, 14(6), 1223-1245.

Denton, S. R., 2007. Achieving sustainable growth in the use of FRP composites in structural rehabilitation. In *Proceedings of conference ACIC-2007.* The University of Bath, Bath, UK. 2-4 April. pp. 50-57.

Duthinh, D., & Starnes, M., 2004. Strength and ductility of concrete beams reinforced with carbon fibre-reinforced polymer plates and steel. *Journal of composites for construction*. *8*(1), pp. 59-69.

El-Refaie, S. A., Ashour, A. F., & Garrity, S. W., 2003. Sagging and hogging strengthening of continuous reinforced concrete beams using carbon fiber-reinforced polymer sheets. *ACI structural journal*. *100*(4), pp. 446-453.

Lee, J.H., 2010. Performance of U-wrap as an anchorage system in externally-bonded FRP reinforced concrete elements. PhD thesis. The Pennsylvania State University, USA.

Lou, T., Lopes, S. M., & Lopes, A. V., 2015b. Neutral axis depth and moment redistribution in FRP and steel reinforced concrete continuous beams. *Composites Part B: Engineering*, 70, 44-52.

Meier, U., Deuring, M., Meier, H. and Schwegler, G., 1993. *CFRP bonded sheets* (pp. 423-434). Elsevier Science, Amsterdam.

Mukhopadhyaya, P., Swamy, N. and Lynsdale, C., 1998. Optimizing structural response of beams strengthened with GFRP plates. *Journal of composites for construction*, *2*(2), pp.87-95.

Oehlers, D. J., Ju, G., Liu, I. S. T., & Seracino, R., 2004. Moment redistribution in continuous plated RC flexural members. Part 1: neutral axis depth approach and tests. *Engineering structures*. *26*(14), pp. 2197-2207.

Oehlers, D. J., 2006. Ductility of FRP plated flexural members. *Cement and Concrete Composites*. *28*(10), pp. 898-905.

Oehlers, D.J., Haskett, M., Ali, M.M. and Griffith, M.C., 2010. Moment redistribution in reinforced concrete beams. *Proceedings of the Institution of Civil Engineers-Structures and Buildings*, *163*(3), pp.165-176.

Santos, P., Laranja, G., França, P. M., & Correia, J. R., 2013. Ductility and moment redistribution capacity of multi-span T-section concrete beams reinforced with GFRP bars. *Construction and Building Materials*, *49*, pp. 949-961.

Silva, P. F., & Ibell, T. J., 2008. Evaluation of moment distribution in continuous fiber-reinforced polymer-strengthened concrete beams. *ACI Structural Journal*. *105*(6), pp. 729-739.

Tajaddini, A., Ibell, T. J., Darby, A. P. and Evernden, M., 2013. A parametric study on moment redistribution in FRP-strengthened continuous RC beams. *In*: *11th International Symposium on Fibre Reinforced Polymer for Reinforced Concrete Structures (FRPRCS-11), 2013: Conference Proceedings.* University of Minho, Guimaraes, Portugal. 24-26 June. pp. 203-204.

Tajaddini, A., 2015. Investigation of moment redistribution in FRP-strengthened RC slabs and T-beams. *PhD thesis*. University of Bath, United Kingdom.

Teng, J. G., Chen, J. F., Smith, S. T., & Lam, L., 2001. *FRP: strengthened RC structures*. Wiley, New York.

Yost, J. R., Gross, S. P., Dinehart, D. W., & Mildenberg, J. J., 2007. Flexural behaviour of concrete beams strengthened with near-surface-mounted CFRP strips. *ACI structural journal*, 104(4).

List of figures:

List of tables